Design of a Two-Phase Molten Salt Natural Circulation Loop based on the Law of Similarity and Preliminary Analysis of Natural Circulation Using OpenFOAM

Won Jun Choi[a], Jae Hyung Park[a], Seung Gyu Hyeon[a], Jinho Song[a], and Sung Joong Kim*[a,b]
[a]*Department of Nuclear Engineering, Hanyang University*
222 Wangsimni-ro, Seongdong-gu, Seoul 04763, Republic of Korea
[b]*Institute of Nano Science and Technology, Hanyang University*
222 Wangsimni-ro, Seongdong-gu, Seoul 04763, Republic of Korea
**Corresponding author: sungjkim@hanyang.ac.kr*

***Keywords : Law of similarity, Molten salt reactor (MSR), Natural circulation, Helium injection**

1. Introduction

Liquid-fueled molten salt reactors (MSRs) are being actively developed due to their attractive features, including high thermal efficiency and inherent safety. In this regard, the i-SAFE-MSR research center was established in South Korea, focusing on the development of a passive molten salt fast reactor (PMFR), an advanced type of MSR [1]. The PMFR incorporates several innovative technologies such as natural circulation operation without reactor coolant pumps, a long-life core design lasting up to 20 years, and reduced radioactive waste by eliminating the graphite moderator. Notably, the natural circulation operation in the PMFR can mitigate risks associated with unpredictable transient events, such as pump damage caused by high temperature and high corrosive molten salt.

However, the PMFR faces a significant challenge related to insoluble fission products (IFPs). These IFPs circulate throughout the primary system along with the liquid fuel, potentially adhering to material surfaces, which can accelerate local corrosion and reduce heat transfer efficiency. To address this issue, the PMFR utilizes an IFP removal system known as the helium bubbling system. When helium bubbles are injected into the reactor via this system, the IFPs attach to the helium bubbles instead of the material surfaces. This process effectively mitigates the negative impacts of IFPs.

Simultaneously, the helium bubbling system provides an additional benefit beyond the removal of IFPs. When helium bubbles are injected into the reactor system, the buoyant force resulting from the density difference between the helium bubbles and the working fluid imparts a driving force for natural circulation. In other words, helium injection enhances the natural circulation performance of the working fluid [2]. This improved circulation performance can increase the available thermal power of the reactor. Additionally, changes in the two-phase flow pattern may influence reactor stability during operation.

To quantitatively evaluate the helium bubbling effect in terms of natural circulation performance, a two-phase natural circulation experiment under molten salt conditions is required. However, it is difficult to conduct the two-phase natural circulation experiment under the actual conditions of the PMFR due to its large scale with an approximate height of 20 meters, high operating temperatures above 600 °C, and the presence of radioactive materials. Therefore, to evaluate the helium bubbling effect via experiment under PMFR-like conditions, it is necessary to design a two-phase molten salt natural circulation loop where the law of similarity is applied. However, information on the relevant similarity criteria for MSRs is insufficient at present.

Thus, in this study, a two-phase molten salt natural circulation loop incorporating the helium injection was designed using the law of similarity. Additionally, a preliminary analysis using OpenFOAM was performed to evaluate the feasibility of natural circulation under the molten salt conditions.

2. Derivation of similarity criteria

To derive the similarity criteria, it is essential to establish a governing equation that accurately represents the target system. The PMFR involves three major phenomena: volumetric heat generation in the liquid fuel, natural circulation of the working fluid, and two-phase flow due to helium injection. To model these phenomena effectively, the drift-flux model was employed.

The drift-flux model treats the dispersed phase (gas) and the continuous phase (liquid) as a unified mixture, rather than analyzing them separately. It generally assumes that velocity differences between the phases occur under thermal equilibrium conditions, allowing for a straightforward explanation of two-phase phenomena [3]. The governing equations based on the drift-flux model, as proposed by Ishii et al., are presented in Eqs. (1)–(4) [4].

$$\frac{\partial \alpha \rho_g}{\partial t} + \nabla\left(\alpha \rho_g u_m\right) = \Gamma_g - \nabla\left(\frac{\alpha \rho_g \rho_l}{\rho_m} V_{gj}\right) \quad (1)$$

$$\frac{\partial \rho_m}{\partial t} + \nabla\left(\rho_m u_m\right) = 0 \quad (2)$$

$$\frac{\partial \rho_m u_m}{\partial t} + \nabla(\rho_m u_m^2) = -\nabla p_m - \rho_m g - f_m - \nabla\left(\frac{\alpha \rho_g \rho_l}{(1-\alpha)\rho_m} V_{gj}^2\right) \quad (3)$$

$$\frac{\partial \rho_m H_m}{\partial t} + \nabla(\rho_m u_m H_m) = \frac{4h_m}{d}(T_s - T_{sat}) - \nabla\left(\frac{\alpha \rho_g \rho_l}{\rho_m} \Delta H_{fg} V_{gj}\right) \quad (4)$$

$$\Gamma_g = \frac{4h_m(T_s - T_{sat})}{d\Delta H_{fg}} \quad (5)$$

Here, α, t, ρ, u, p, Γ_g, V_{gj} represent void fraction, time, density, velocity, pressure, vapor source term, and drift velocity, respectively. Additionally, g, f, H, h, d, T_s, T_{sat}, ΔH_{fg} denote gravitational acceleration, friction factor, enthalpy, heat transfer coefficient, hydraulic diameter, solid (wall) temperature, saturation temperature of working fluid, and enthalpy of vaporization, respectively. The subscripts m, g, and l refer to the mixture, gas-phase, and liquid-phase, respectively.

Eqs. (1)–(4) represent the vapor continuity equation (continuity equation for dispersed phase), the mixture continuity equation, the mixture momentum equation, and the mixture energy equation, respectively. The last term on the right-hand side of each equation except for Eq. (2) is diffusion term derived from the velocity differences between two-phases. Additionally, Eq. (5), which is included in Eq. (1), describes the vapor source term resulting from phase changes.

These equations were pertinently modified to simulate the PMFR. The original vapor continuity equation included a vapor source term accounting for phase changes. However, in the PMFR, the two-phase flow is only caused by helium injection without phase change. Therefore, the vapor source term was revised as shown in Eq. (6) where Q and V are volumetric flow rate and volume of the two-phase region (e.g. riser channel), respectively. Except for the vapor source term, the continuity equations identical to Eqs. (1) and (2) were utilized to derive the similarity criteria.

$$\Gamma_g = \frac{\rho_g Q_g}{V} \quad (6)$$

Eq. (7) presents the integrated two-phase momentum equation. According to Donghua et al., the integrated momentum equation takes the same form for both single-phase and two-phase flows as the diffusion term due to velocity differences between phases and the advection term due to fluid movement are eliminated during the procedure of integration over the entire loop [5]. Thus, in this study, the integrated two-phase momentum equation as shown in Eq. (7) was utilized.

$$\rho_r \sum_i \left(l_i \frac{a_r}{a_i}\right) \frac{\partial u_r}{\partial t} = \Delta\rho g l_{hc} - \frac{1}{2}\rho_r u_r^2 \sum_i \left(\left(\frac{\rho_r}{\rho_i}\right)\left(\frac{a_r}{a_i}\right)^2 \left(\frac{fl}{d_h} + k\right)_i\right) \quad (7)$$

The original energy equation based on the drift-flux model, as shown in Eq. (4), was established to describe two-phase heat transfer due to phase change. Therefore, the original energy equation includes parameters related to phase change, such as saturation temperature and enthalpy of vaporization. However, the PMFR involves two-phase phenomena due to helium injection while maintaining the working fluid in a single-phase state. Consequently, Eq. (8), which represents the single-phase fluid energy equation, was utilized to derive the similarity criteria. In the Eq. (8), volumetric heat generation term (q''') was included to reflect the characteristics of liquid fuel in the PMFR.

$$\rho_l C_p \frac{\partial T_l}{\partial t} + \rho_l C_p u_l \nabla T_l = q''' + \frac{4}{d} h(T_s - T_l) \quad (8)$$

The coefficients of each nondimensionalized equation, known as similarity criteria, are derived as shown in Eqs. (9)–(12) by nondimensionalizing the modified governing equations. Although each variable in the coefficients has its own unit, the coefficients themselves are dimensionless because the units in the numerator and denominator cancel each other out.

$$\frac{\partial \alpha \rho_g^*}{\partial t^*} + \nabla^*(\alpha \rho_g^* u_m^*) = \left(\frac{\Gamma_{g0}\, l_0}{\rho_{g0}\, u_{m0}}\right)\Gamma_g^* - \left(\frac{V_{gj0}\, \rho_{l0}}{\rho_{m0}\, u_{m0}}\right)\nabla^*\left(\frac{\alpha \rho_g^* \rho_l^*}{\rho_m^*} V_{gj}^*\right) \quad (9)$$

$$\frac{\partial \rho_m^*}{\partial t^*} + \nabla^*(\rho_m^* u_m^*) = 0 \quad (10)$$

$$\rho_r^* \sum_i \left(l_i^* \frac{a_r^*}{a_i^*}\right) \frac{\partial u_r^*}{\partial t^*} = \left(\frac{\Delta\rho_{mo}\, g_0\, l_0}{\rho_{m0}\, u_{m0}^2}\right)\Delta\rho^* g^* l_{hc}^* - \frac{1}{2}\rho_r^* u_r^{*2} \sum_i \left(\left(\frac{\rho_r^*}{\rho_i^*}\right)\left(\frac{a_r^*}{a_i^*}\right)^2 \left(\frac{fl}{d_h} + k\right)_i\right) \quad (11)$$

$$\frac{\partial T_l^*}{\partial t^*} + u_l^* \nabla^* T_l^* = \left(\frac{l_0\, q'''}{C_p\, \Delta T_0\, u_{m0}\, \rho_{l0}}\right) + \left(\frac{4hl_0}{d\, u_{m0}\, C_p\, \rho_{l0}}\right)(T_s^* - T_l^*) \quad (12)$$

Consequently, five similarity criteria were derived as shown in Eqs. (13)–(17). These criteria are the gas injection number, drift velocity number, Richardson number, heat source number, and Stanton number, respectively. The subscript R denotes the ratio between the prototype (PMFR) and the model (two-phase molten salt natural circulation loop). The detailed information on the prototype (PMFR) such as V_{gj0}, which is related to the two-phase flow regime and h, which is related to heat

transfer efficiency was not concretized at present. Therefore, only Eqs. (13), (15), and (16) were utilized in the design of two-phase molten salt natural circulation loop in this study.

$$\left(\frac{\Gamma_{g0}\, l_0}{\rho_{g0}\, u_{m0}}\right)_R = 1 \tag{13}$$

$$\left(\frac{V_{gj0}\, \rho_{l0}}{\rho_{m0}\, u_{m0}}\right)_R = 1 \tag{14}$$

$$\left(\frac{\Delta\rho_{m0}\, g_0\, l_0}{\rho_{m0}\, u_{m0}^2}\right)_R = 1 \tag{15}$$

$$\left(\frac{l_0\, q'''}{C_p\, \Delta T_0\, u_{m0}\, \rho_{l0}}\right)_R = 1 \tag{16}$$

$$\left(\frac{4hl_0}{d\, u_{m0}\, C_p\, \rho_{l0}}\right)_R = 1 \tag{17}$$

3. Design of experiment loop

The two-phase molten salt natural circulation loop was designed using both the design parameters of the prototype as shown in Table 1 and the derived similarity criteria. Since the working fluids differ between the PMFR (NaCl(0.363)-KCl(0.255)-UCl_3(0.382)) and the two-phase molten salt natural circulation loop (HITEC salt: KNO_3(0.53)-$NaNO_2$(0.40)-$NaNO_3$(0.07)), the material property ratios, such as density and specific heat, cannot be canceled out in the similarity criteria derived above. Additionally, if the amount of helium injection becomes too large in the PMFR, it can cause the reactor instability during operation. Therefore, helium injection is typically limited to a void fraction of 1%. Based on the pressure balance equation, it was determined that a helium injection rate of 200 L/min (lpm) results in a 1% helium void fraction in the riser channel of the PMFR.

Based on the gas injection number given in Eq. (13), the helium injection rate for the loop was designed to be 0.011 lpm to achieve the void fraction of 1 %. The Richardson number, as described in Eq. (15), provides constraints on system velocity. According to the heat source number in Eq. (16), the two-phase molten salt natural circulation loop requires the thermal power of about 15 kW to simulate the active core in the PMFR. Consequently, the design parameters for the model are presented in Table 1.

Table 1. Design parameters of prototype and model

Design parameters	Prototype (PMFR)	Model (Expt. loop)
Pressure [atm]	1	1
Core inlet Temperature [°C]	500	200
Core height [m]	2	1
Temperature differences (core in/outlet) [°C]	190	100
Diameter at core inlet [m]	2	0.02118
Area at core inlet [m^2]	3.14159	0.00035
Volume of riser channel [m^3]	5.08938	0.00025
Velocity of system [m/s]	0.215	0.12098
Power [W]	3.00E+08	14861.89
Helium injection rate [m^3/s]	0.00333 (= 200 lpm)	1.81788E-07 (= 0.011 lpm)
Core volume [m^3]	6.28319	0.00035
Volumetric heat [W/m^3]	4.77E+07	42182480.87
Riser height [m]	18	0.7
Riser diameter [m]	0.6	0.02118
Riser width [m^2]	0.28274	0.00035

4. Preliminary calculations

Based on the design parameters of the two-phase molten salt natural circulation loop presented in Table 1, the geometry was created using SpaceClaim for computational fluid dynamics (CFD) analysis, as shown in Fig. 1. The geometry includes three heating sections and two cooling sections. The mesh was generated using the polyhedral type in Ansys Meshing, resulting in a total of 282,535 cells. The mesh was then converted to the OpenFOAM-compatible format using the utility of fluent3DMeshToFoam.

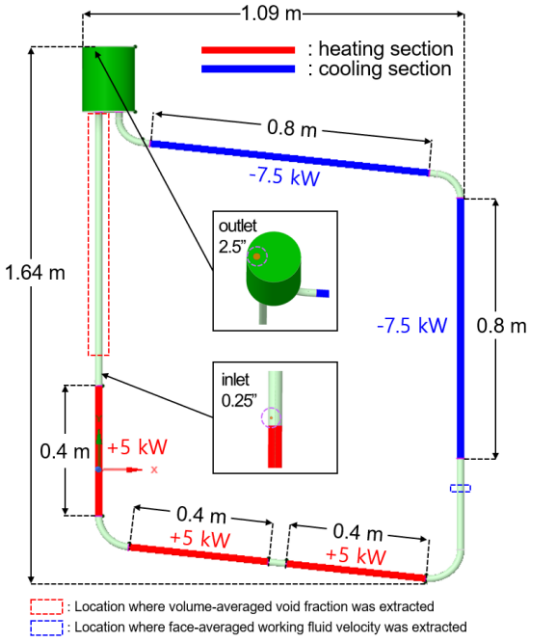

Fig. 1. 3D schematic of experiment loop

The numerical analysis was executed using OpenFOAM (version 9), which offers a wide range of solvers and utilities designed to simulate various physical phenomena. In this study, the

multiphaseEulerFoam solver, which is suitable for systems with multiple compressible fluid phases, was used to simulate two-phase natural circulation. The transient analysis was conducted using the PIMPLE algorithm, a pressure-velocity coupling method. The Schiller-Naumann model, which is widely used for calculating drag forces in two-phase flows, was chosen as the drag flux model. Key parameters used in the OpenFOAM calculation are listed in Table 2.

Table 2. Simulation parameters in OpenFOAM

Parameters	Values
Simulation	
Solver	multiphaseEulerFoam
Momentum transport	laminar
Time step	0.001~0.003
Iteration and discretization	
Iterative solver	PIMPLE (Pressure – Velocity coupling algorithm)
Time Schemes	Euler (Transient analysis)
Gradient Schemes	Gauss linear
Laplacian Schemes	Gauss linear uncorrected
Drag flux model	Schiller-Naumann
	segregated
Temperature boundary condition	
Heating section	externalWallHeatFluxTemperature (5 kW per heater)
Cooling section	externalWallHeatFluxTemperature (-7.5 kW per cooler)
Adiabatic walls	zeroGradient

ParaView 5.10.1 was used for post-processing. Figs. 2 (a) and (b) show the analysis domains for cases without and with helium injection, respectively. The change in velocity of the working fluid according to helium injection was analyzed. Additionally, the average void fraction was evaluated in the helium injection case. The transient simulation was run until only 500 seconds, as the two-phase transient calculation required significant computational time. Consequently, the initial state of natural circulation was examined in this study.

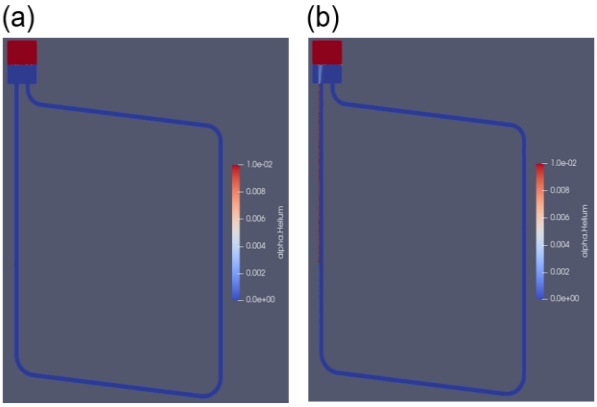

Fig. 2. Natural circulation simulation: (a) without helium injection and (b) with helium injection

Fig. 3 presents a graph of the face-averaged working fluid velocity over time, comparing cases with and without helium injection. The face-averaged working fluid velocity was extracted at the location marked by the blue dotted box in Fig. 1. Given that the helium injection rate was very low at 0.011 lpm, no significant change in flow rate was observed with or without helium injection.

However, despite some fluctuations, it was noted that natural circulation flow rates were generally higher when helium was injected compared to when it was not. By averaging the data of face-averaged working fluid velocity from 300 to 500 seconds, the helium injection case exhibited the faster working fluid velocity compared to the case without helium injection about 2.09 %. Nonetheless, it is unclear whether the value of 2.09 % came from the actual helium injection effect or is merely a consequence of numerical instability. Therefore, this study has a room for improvement such as performing the additional simulation beyond the 500 seconds.

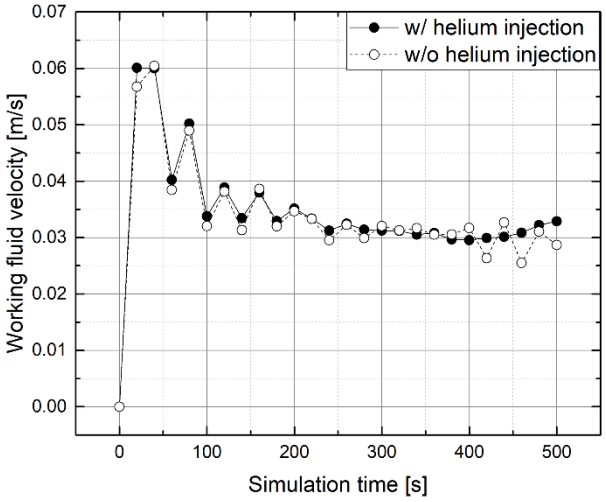

Fig. 3. Face-averaged working fluid velocity with and without helium injection, as extracted from the location of the blue dotted box shown in Fig. 1

Fig. 4 exhibits the change in void fraction over time with helium injection. The volume-averaged void fraction data were extracted from the location marked by the red dotted box in Fig. 1. By averaging the void fraction data from 300 to 500 seconds, a time-averaged and volume-averaged void fraction of 0.191% was obtained. However, the void fraction did not reach a steady state since the calculation was only run until 500 seconds. The time- and volume-averaged void fraction was found to be lower than the target void fraction of 1%. This discrepancy is interpreted as a distortion due to differences in the two-phase flow patterns between the prototype and the model. Additionally, the omission of the drift velocity number when applying similarity law could be another reason for the distortion.

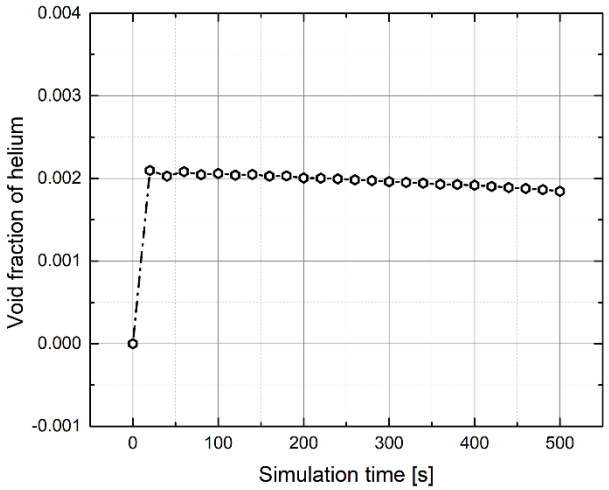

Fig. 4. Volume-averaged void fraction in the helium injection case, as extracted from the location of the red dotted box shown in Fig. 1

5. Summary and conclusion

This study focused on the development of a scaled-down two-phase molten salt natural circulation loop using the law of similarity to simulate the PMFR. To evaluate the helium bubbling effect in terms of natural circulation, preliminary analysis was conducted using OpenFOAM. The major findings of this study can be summarized as follows:

- ✓ The similarity criteria were derived from the nondimensionalization of governing equations based on the drift-flux model.
- ✓ The gas injection number, Richardson number, and heat source number were utilized during the design of two-phase molten salt natural circulation loop
- ✓ According to heat source number, the thermal power of loop needs about 15 kW to simulate the thermal power of PMFR
- ✓ The helium injection case exhibited the faster working fluid velocity compared to the case without helium injection about 2.09 %
- ✓ The time- and volume-averaged void fraction of 0.191 % was found to be lower than the target void fraction of 1% due to distortion of similarity law.

However, this study has room for improvement, such as applying more precise similarity law and performing additional preliminary analysis. Consequently, a more advanced experimental loop will be designed using improved similarity law and further preliminary analysis. Based on this advanced loop, a two-phase natural circulation experiment, including helium injection, will be conducted. This experiment will provide valuable data on two-phase natural circulation under molten salt conditions and offer critical insights to optimize the design and operational strategies of the PMFR.

Acknowledgments

This research was supported by the National Research Foundation of Korea (NRF) and funded by the ministry of Science, ICT, and Future Planning, Republic of Korea (grant numbers NRF-2021M2D2A2076382). Additionally, this work was also supported by the Human Resources Development of the Korea Institute of Energy Technology Evaluation and Planning (KETEP) grant funded by the Korea government Ministry of Knowledge Economy (RS-2024-00439210).

REFERENCES

[1] Park, J. H., Choi, W., Lim, J., Kim, T., Kim, Y., Yoon, Y., ... & Kim, S. J. (2022). Design Concepts and Requirements of Passive Molten Salt Fast Reactor (PMFR). In *Transactions of the Korean Nuclear Society Spring Meeting* (pp. 1-6).
[2] Choi, W. J., Park, J. H., Lee, J., Im, J., Cho, Y., Kim, Y., & Kim, S. J. (2024). Experimental and numerical assessment of helium bubble lift during natural circulation for passive molten salt fast reactor. *Nuclear Engineering and Technology*, *56*(3), 1002-1012.
[3] Goda, H., Hibiki, T., Kim, S., Ishii, M., & Uhle, J. (2003). Drift-flux model for downward two-phase flow. *International journal of heat and mass transfer*, *46*(25), 4835-4844.
[4] Ishii, M., & Kataoka, I. (1984). Scaling laws for thermal-hydraulic system under single phase and two-phase natural circulation. *Nuclear Engineering and Design*, *81*(3), 411-425.
[5] Lu, D., Xiao, Z., & Chen, B. (2010). A new method to derive one set of scaling criteria for reactor natural circulation at single and two-phase conditions. *Nuclear Engineering and Design*, *240*(11), 3851-3861.